Cold Regions Science and Technology 211 (2023) 103850

Contents lists available at ScienceDirect

Cold Regions Science and Technology

journal homepage: www.elsevier.com/locate/coldregions

The effects of temperature on shallow borehole NMR measurements in permafrost

Taylor D. Sullivan *, Andrew D. Parsekian

University of Wyoming Geology & Geophysics, 1000 E. University Ave., Laramie, WY 82071, United States of America

ARTICLE INFO

Keywords:
Nuclear magnetic resonance
Unfrozen water
Temperature dependence
Permafrost

ABSTRACT

High fidelity observations of the amount and state of water within permafrost help constrain the seasonal behavior of soil moisture and the effects of soil moisture on the surface energy balance. This work emphasizes the necessity for temperature-specific calibrations of low-frequency borehole NMR measurements. Constraining the effects of temperature on NMR signatures will allow for more reliable NMR inspection of hydrogeochemical parameters in permafrost ecosystems. We find that calibration at typical laboratory temperatures (20 °C) and subsequent measurement at typical permafrost active layer temperatures (~0 °C) can result in an 18% bias in reported NMR water content values, and therefore temperature compensation is required under most scenarios. This is particularly important for active layer conditions that may include steep vertical temperature gradients. Similarly, seasonal time-lapse measurements of permafrost active layer may encounter substantial soil temperature variations which would also require temperature compensation on the observed NMR water content estimate.

1. Introduction

Quantifying the response of permafrost thaw to warming atmospheric temperatures requires accurate characterization of the active layer of permafrost—the near-surface zone that seasonally freezes and thaws (Romanovsky and Osterkamp, 2000; Van Everdingen, 1998). The amount of unfrozen water, θ (expressed herein as the fraction of the volume of water to the volume of the total sample volume, $\theta = V_w/V_T$), in cryotic soils depends on physical, chemical, and mineralogical soil characteristics including surface area, solute concentration, temperature, confining pressure, initial water content, and surface chemistry of the soil matrix (Anderson and Tice, 1973). Knowledge of the state of water within the active layer—be it bound by capillary or adsorptive forces to soil particles, mobile within soil pores, or frozen in ice—bolsters understanding of the functional relationship between the soil freezing characteristic curve and the soil moisture characteristic curve (Tian et al., 2018).

Reliable and repeatable quantification of the amount of liquid water within and below the permafrost active layer is important for characterizing hydrological processes and detecting permafrost degradation (Jorgenson and Osterkamp, 2005; Romanovsky and Osterkamp, 2000; Wlostowski et al., 2018). Since the 1970s, nuclear magnetic resonance (NMR) has been employed to study unfrozen water in freezing and thawing soils (Anderson and Tice, 1973; Smith and Tice, 1988). NMR yields information pertaining to soil wetness, pore-scale geometry, and surface mineralogy by probing hydrogen nuclei of water molecules within a soil matrix. Importantly, NMR is the only geophysical measurement that directly measures water, meaning no petrophysical transforms are needed to convert signal strength to volumetric water content – petrophysical transformations are not required, only an instrument calibration in a water tank is needed to scale fractional water contents observed in formations (Behroozmand et al., 2015; Müller-Petke and Yaramanci, 2015; Walsh et al., 2013). To perform a calibration, the NMR signal measured with the tool in a water filled chamber is set as the factor to which all measurements in geologic formations are scaled. The calibration calculation assumes that the amplitude of the NMR response is directly proportional to the number of hydrogen nuclei present within the sensitive zone of the instrument, the sensitive zone is static, and that the temperature of the water within the sample is the same as the temperature of the water in the calibration chamber.

The concept of borehole NMR started with large, truck-mounted NMR logging instrumentation conceived in the 1960s (Brown and Gamson, 1960). In recent decades, portable borehole-deployable NMR probes, which use low-field strength and - therefore low-excitation-

* Corresponding author.
E-mail addresses: taylor.d.sullivan@erdc.dren.mil (T.D. Sullivan), aparseki@uwyo.edu (A.D. Parsekian).

https://doi.org/10.1016/j.coldregions.2023.103850
Received 5 April 2022; Received in revised form 27 February 2023; Accepted 3 April 2023
Available online 6 April 2023
0165-232X/Published by Elsevier B.V.

frequency measurements have allowed for high depth-resolution (25 cm) soil moisture observations (Walsh et al., 2013). The major advantages of these low-frequency NMR measurements in groundwater investigations include the ability to operate in small-diameter, hand-dug temporary boreholes, and the portable nature of the instruments that enables easy access to remote field sites (Walsh et al., 2013).

There are two key temperature-related considerations related to borehole NMR measurements in permafrost environments, and particularly the active layer. First, NMR instruments deployed in permafrost regimes may encounter steep vertical temperature gradients depending on local geology and surface conditions. Second, calibrations may be done under lab conditions (~20 °C), but then measurements may be made at permafrost field temperature (~0 °C). Time lapse studies may face further challenges since the active layer field temperature varies through seasons.

It is known that net magnetization - and therefore NMR response - is inversely proportional to temperature (Bloch, 1946). In freezing soils, the magnitude of the NMR response from hydrogen nuclei depends on temperature due to (1) fundamental thermodynamic and electromagnetic properties of hydrogen nuclei (Grebenkov, 2007; Holtzer, 1954; Rabi, 1937) and (2) the phase change of water molecules from liquid to solid during freeze/thaw (Kass et al., 2017; Smith and Tice, 1988). NMR observations with sample temperatures spanning from 1 to 373 K reliably demonstrate this sensitivity (Bloch, 1946; A. R. Tice et al., 1978) that arises from a balance of aligning influences, i.e. magnetic field strength, and scattering influences, i.e. the effect of temperature, within a sample (Bloch, 1946; Brown and Gamson, 1960).

Recent in situ permafrost NMR studies acknowledge this temperature dependence and closely monitor sample temperature; however, calibration correction factors to account for vertical gradients or temporal changes are not reported. Kleinberg and Griffin (2005) acknowledge the large temperature gradients within permafrost soils on the North Slope of Alaska; however, they do not mention temperature-specific calibration of their 2.2 MHz borehole NMR at depths up to 400 m. Borehole NMR investigations within the active layer of permafrost (where temperatures at the surface range from >15 °C in the summertime to less than −15 °C in the winter (Douglas et al., 2020) are becoming more apparent in scientific literature. Kass et al. (2017) use low-frequency, portable NMR to estimate water contents and hydraulic conductivity of active layer soils in Alaskan boreal forests and report that temperatures were uniform within the soil column (between −1 °C and − 2 °C during the time of measurement). Minsley et al. (2016) and James et al. (2021) conducted similar investigations of active layer water content in regions of discontinuous permafrost, although calibration corrections are not reported.

In order to be able to reliably interpret low-frequency NMR logging data in permafrost environments, the overarching research question that we seek to answer, [Q1], is: How does temperature affect NMR measurements under the circa-cryotic conditions of permafrost active layer soils? We hypothesize that temperature effects on the NMR response produce a water content bias that is non-negligible, particularly when considering steep temperature gradients and time-lapse measurements. We hypothesize the following temperature-dependent internal (i.e., on the instrument) and external (i.e., in the water within the sensitive volume) factors may have a control on measured water content:

- H1: As the internal magnet temperature goes down, the field strength goes up thereby *pushing the sensitive zone farther into the formation* than where it was calibrated.
- H2: As the internal magnet temperature goes down, the field strength goes up thereby changing the slope of the field gradient and *increasing the width of the sensitive zone* compared to the calibrated value.
- H3: NMR signal amplitude within a water sample varies more than would be expected by the standard model.
- H0: The null hypothesis is that only NMR response within liquid water inside the sensitive volume control temperature dependance.

Our results demonstrate that going from a calibration temperature of 20 °C to field conditions of 0 °C produces an 18% bias in water content. While it is possible to simply calibrate the instrument to 0 °C, that would only be useful if the ground temperatures are isothermal – otherwise the possibility for steep vertical temperature measurements makes correction desirable across the depth log. The temperature response is instrument-specific, so a temperature correction factor should be assessed for each instrument prior to non-isothermal measurements.

2. Background and theory

NMR is useful to geophysicists because the technique provides a direct measurement of water volume. NMR surveys may be made in three geometries: surface-NMR leverages the Earth's natural background magnetic field and measures NMR response as depth soundings, and lab- and borehole-NMR utilize permanent magnets to establish the background magnetic field (Behroozmand et al., 2015). This study focuses on borehole and lab NMR. NMR probes the spin magnetic moment, an intrinsic physical property of hydrogen protons. Subjected to a magnetic field, the spin magnetic moments of hydrogen protons align with the applied field and precess about the static magnetic field at the Larmor frequency (Bloch, 1946):

$$f_L = \frac{\omega_L}{2\pi}; \omega_L = \gamma \boldsymbol{B_0} \tag{1}$$

The net magnetization of the sample volume at thermal equilibrium depends on the number of spins (hydrogen protons), temperature, and the applied magnetic field strength (Bloch, 1946; Waller, 1932).

The lab-NMR and borehole NMR instruments considered in this study utilize the Carr-Purcell-Meiboom-Gill (CPMG) pulse sequence to conduct measurements (Carr and Purcell, 1954; Meiboom and Gill, 1958). This pulse sequence utilizing 180^o refocusing pulses was developed to rephase proton spins in solids subjected to a heterogeneous magnetic field. The maximum value of the CPMG exponential decay curve—the same value as the maximum value of the free induction decay, FID, pulse sequence—is calibrated to a sample of entirely liquid water at some equilibrium temperature.

$$\theta_{NMR} = \frac{V_{NMR}}{V_S} \tag{2}$$

here, θ_{NMR} is NMR-estimated water content, V_{NMR} is the true volume of water in the sample, and V_S is the volume of the measured sample. Sample temperature affects NMR signal strength due to diffusion and water molecule density (Grebenkov, 2007).

The amount of NMR-sensed water during freezing depends on the amount of unfrozen water and the sample temperature (Kass et al., 2017; Kruse et al., 2018). The phase change of liquid water to ice manifests as a (i) overall reduction in the NMR signature due to the displacement of liquid water with ice as ice expands 9% upon freezing, and (ii) rapidly-decaying echo sequence from near-freezing ice (Kruse et al., 2018). Subjected to a fleeting magnetic field, ice elicits a relaxation signature up to 50 μs which influences the NMR signal (Kruse et al., 2018; Watanabe and Wake, 2009); however, such short relaxation times are not measurable using current shallow-borehole NMR instrumentation.

The standard model depicts the net magnetization of the spin magnetic moment of hydrogen protons in water, $\boldsymbol{M}_0$, as a function of sample temperature, a constant number of spin magnetic moments within the sensitive zone, magnetic field strength, and temperature-independent physical constants. In water, this relationship reduces to (simplified Eq. (2)):

$$\text{Model}_{\text{standard}} = \boldsymbol{M}_0 = \frac{n\gamma^2\hbar^2}{4K_B T}\boldsymbol{B_0} \tag{3}$$

where n = the number of protons per unit volume, γ = proton gyromagnetic ratio, $\hbar$ is the reduced Planck's constant, T is temperature, and K_B is the Boltzmann constant.

To better understand the effect of water density changes with temperature on the number of hydrogen protons, n, within the sample volume, V, we model the relationship between water density and temperature:

$$\text{Model}_{\rho(T)} = \boldsymbol{M}_0 = \frac{n(\rho_w(T))|_V \gamma^2\hbar^2}{4K_BT}\boldsymbol{B_0} \quad (4)$$

We calculate the contribution of the change in the number of water molecules within the sample volume due to density by fitting water density observations from 0 to 20 °C (Ground Water Manual Hydrologic Data and Internet Resources, 1977) to a 3rd order polynomial.

$$n(T) = \rho_w(T) = \left(1.57\times10^{-7}\right)T^3 - \left(1.40\times10^{-4}\right)T^2 + 0.041T - 3.04 \quad (5)$$

The magnetic field of the tool becomes stronger under colder temperatures, thereby causing the zone of sensitivity to move slightly farther from the instrument, and to become slightly wider. This effect of changing sampling volume due to temperature-dependent magnetic field strength was determined empirically by measuring a radial cross-section of the probe magnetic field strength at 2 cm spatial resolution and equilibrium temperatures of 20 °C, 10 °C, and −8 °C. These field strength measurements were used to determine the sensitive radius of the probe, i.e. the radius at which $\boldsymbol{B} = \frac{\gamma}{\omega_L}$ (from Eq. (1)) where ω_L is equal to the measurement frequency of the instrument. The modeled increase in instrument sensitivity with decreasing temperature due to the changing sensitive volume is given by Eq. (6).

$$\text{Model}_{SV(T)} = \boldsymbol{M}_0 = \frac{n(\rho_w(T), V(T))\gamma^2\hbar^2}{4K_BT}\boldsymbol{B_0} \quad (6)$$

3. Methods

To test the temperature dependence of NMR measurements, borehole NMR (Dart by Vista Clara, Mukilteo, WA) measurements were completed in a − 20 °C to 20 °C water bath located in the Cold Regions Research Engineering Lab Alaska Research Office cold rooms in Fairbanks, AK. The experimental setup consisted of the NMR probe in a water filled 50 gal plastic bin secured by clamping the top of the probe to the ceiling and centralized through a 5 cm diameter hole cut through plywood affixed to the top of the bin (Supplemental Fig. S1 and Fig. S2). Room and water temperatures were monitored using a four-channel Hobo temperature logger with one sensor 10 cm above the tank assembly and three sensors located 10 cm, 30 cm, and 50 cm from the bottom of the water tank. The entire water tank was wrapped with aluminum foil (except for the hole for the probe at the top) to serve as a Faraday cage around the sensitive zone of the instrument and limit ambient electromagnetic noise. The temperature of the cold room was adjusted incrementally from 20 °C to −20 °C over a two-month period during which the room temperature was set to the desired level and water temperature was allowed 12–24 h to equilibrate with the room temperature.

NMR measurements were recorded every hour. We monitored water temperature, noise in the raw data, battery voltage, and quality factor (i.e., a resonator's bandwidth relative to its center frequency). Borehole NMR measurements utilized two frequencies to optimize signal to noise ratio, and results were weighted according to the noise levels of each frequency. NMR measurements in the water tank were made at 426,270 Hz and 478,271 Hz using a 50 μs excitation pulse length, 800 μs echo spacing, 10 s relaxation time, and 50 averages. Observed noise in the measurements was <3%.

To isolate the effect of the NMR probe temperature from the water temperature, we used the Corona NMR (Vista Clara, Mukilteo, WA) lab instrument to produce conditions where the instrument temperature could be constant while varying the water temperature (Supplemental Figs. S3-S5). We performed triplicate calibration measurements on a room temperature (20 °C), water filled plastic cylinder (7 cm diameter, 15 cm length, Supplemental Fig. S3b), then placed the sample in a − 14 °C freezer until the onset of visible ice crystallization, and then removing the sample (0 °C) from the freezer and monitoring the NMR response every 60 min until the sample reached room temperature. Thermistors were affixed on the top and bottom of the cylinder to monitor sample temperature during warming. Though lab- and borehole-NMR operate on the same physical principles, have similar background magnetic field strengths, and use similar electronic components, they have instrument-specific water content calibrations as a function of temperature due to differences in their magnetic fields since the borehole tool is "outward focused" and the lab instrument is "inward focused" (Tice et al., 1988).

To isolate the effect of sample temperature on NMR signal amplitude from the effect of probe temperature (controlling background magnetic field strength), the borehole NMR probe was insulated in a 10 cm diameter capped PVC pipe (Supplemental Fig. S5) and inserted into a tank of near-freezing water. The NMR control unit, computer, and chargers were kept in a separate room from the probe. The probe temperature slowly decreased from 20 °C to 2 °C over the course of 6 h, and the NMR-sensed water contents were recorded. To further understand how the internal NMR probe's magnetic field is spatially affected by temperature changes, we measured a radial cross section map of magnetic field strength of the NMR probe at 2 cm spatial resolution using a Hall probe (Gauss Meter 300 from Alpha Labs, UT; 0.1 Gs resolution below 20,000 Gs) at different ambient temperatures. Measurement position was marked on a stationary grid for each measurement, and total magnetic field strength was calculated using the vector sum of measurements in the horizontal (x, perpendicular to NMR probe), vertical (y, parallel with NMR probe), and vertical (into page, orthogonal to x and y) directions. The probe was measured in Faraday-cage-like conditions at 20 °C and − 8 °C.

4. Results

4.1. The net effect of temperature on instrument and sample

In Fig. 1, we show the water contents reported during the cooling experiment where both the probe and water sample temperatures are varied together. The observed battery voltage reflects cyclic charging of two parallel 130 Ah, deep-cycle marine batteries plugged into a 15 A computer charger metered by a 9 A DC inverter for minimal measurement noise. Computer and battery chargers were placed outside of the metal-lined cold room. The effect of temperature on bulk water showed some predicted results and some surprises. Both lab-NMR and borehole-NMR report 100% water content at 20 °C (the standard calibration temperature), but they both overestimate water content as the sample temperature decreases: lab-NMR overestimates by 10% at 0 °C, and borehole NMR overestimates by 18% at 0 °C (Fig. 1).

NMR observations on bulk water over a range of temperatures appear to be linear, and follow the Curie formula for sample magnetization (standard model in Fig. 2), increased magnetic field strength with temperature which effects the Larmor frequency and sensitive volume for borehole NMR, or water density changes with temperature fail to explain the variation in NMR-sensed total water content with temperature. NMR magnetization as a function of temperature from −20 to 20 °C along with models accounting for water density and instrument sensitive volume are shown below. Eq. (6) is labeled, "$\text{Model}_{SV(T)}$", in Fig. 2. Fig. 2 also includes theoretical models accounting for sample volume, water density, and magnetic field strength. Fig. 3 also shows the empirically fit models that could be used to normalize data acquired at a range of temperatures.

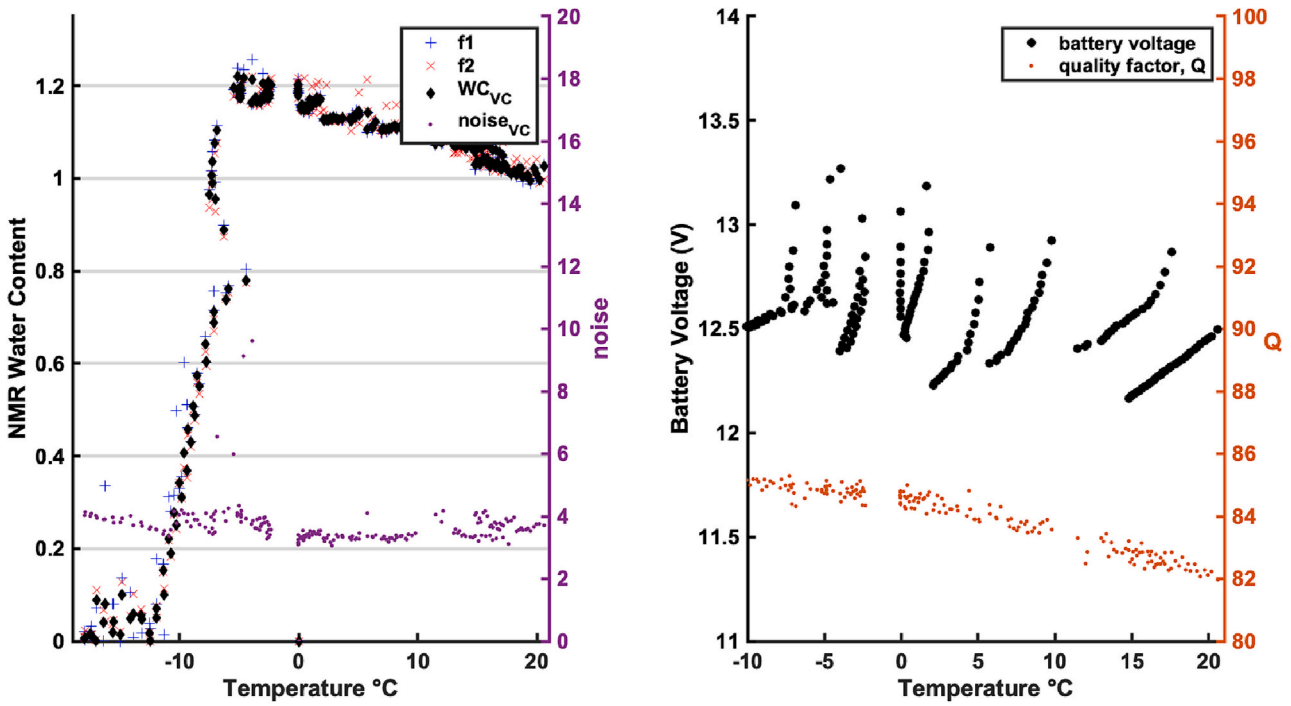

Fig. 1. Dart measured (a) water content, noise, (b) battery voltage, and Q vs. temperature.

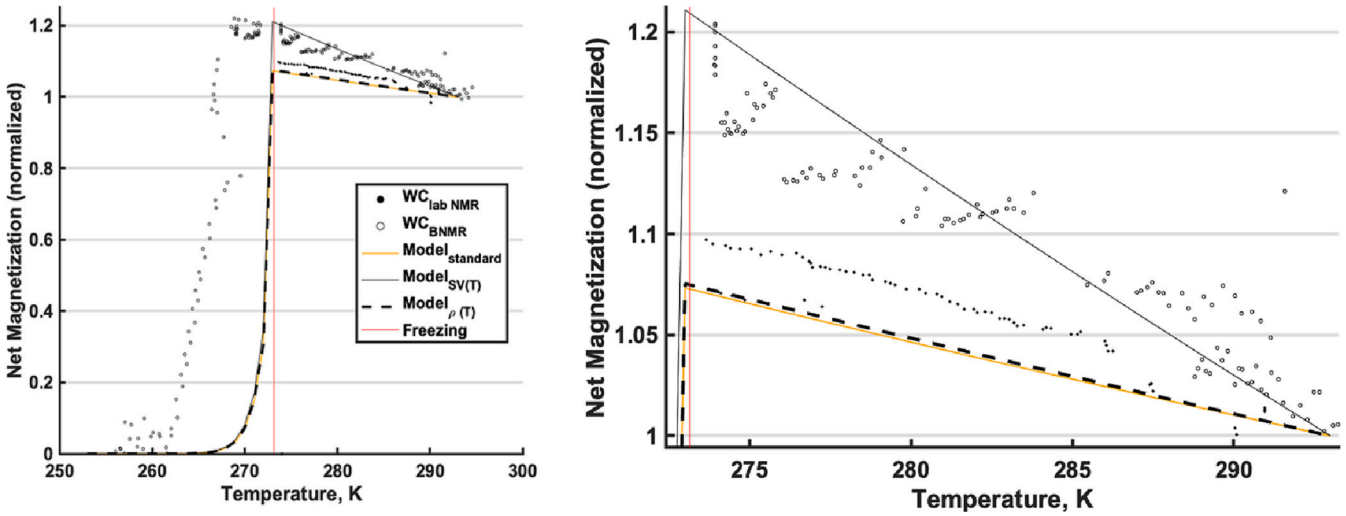

Fig. 2. Lab-, borehole-, and theoretical NMR response as a function of temperature. "$Model_{standard}$", "Model $_{\rho(T)}$", and "$Model_{SV(T)}$" corresponds to Eqs. (3), (4), and (6), respectively.

4.2. Effect of temperature on sample only

In this test, the temperature of the lab-NMR magnet does not change over time while the sample temperature increases. Fig. 2 shows water content observations on a warming cylindrical sample measured with lab-NMR (solid markers) that approximately follow the slope of the standard model.

4.3. The effect of temperature on magnetic field strength

Here we explored how the magnetic field strength varied when changing only the temperature of the probe. Fig. 4 shows a 2D radial-cross-section of the magnetic field strength at room temperature and the changes in magnetic field strength with temperature. Colder temperatures increased magnetic field strength in some areas and decreased it in others—possibly due to highly-temperature dependent heterogeneities of the magnetic field close to the tool. A potentially significant result of changing magnetic field strength with temperature is a change in the volume of the sensitive zone. The sensitive zone is defined by the thin cylindrical shell with a radius equal to the distance from the probe where the Larmor frequency (a function of magnetic field strength, Eq. (1)) equals that of the instrument pulse. The sensitive volume increased with decreased temperatures and increased magnetic field strength (Fig. 5a). The linearly extrapolated relationship between sensitive volume and temperature is depicted in Fig. 5b.

4.4. Effect of temperature changes on the NMR probe

As shown in Fig. 6, when water temperature is held constant and probe temperature decreased from 20 °C to 2 °C, the NMR-sensed water

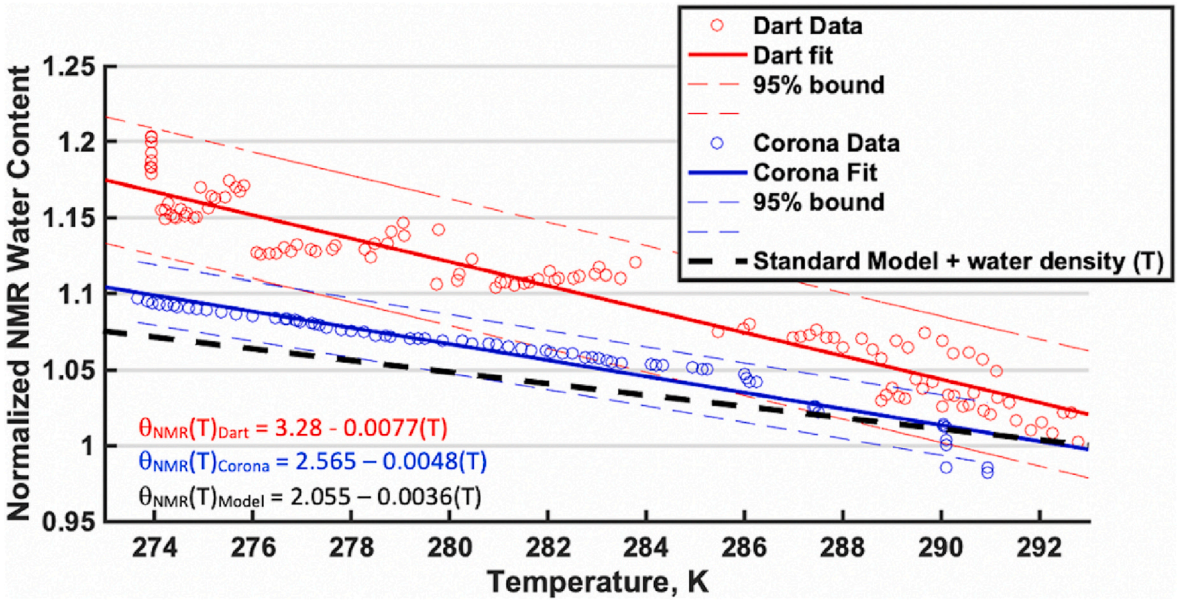

Fig. 3. Borehole (Dart) and lab (Corona) NMR data with fits and 95% confidence bounds. Lab measurements are plotted alongside the model fit of NMR net magnetization (Eq. (3)).

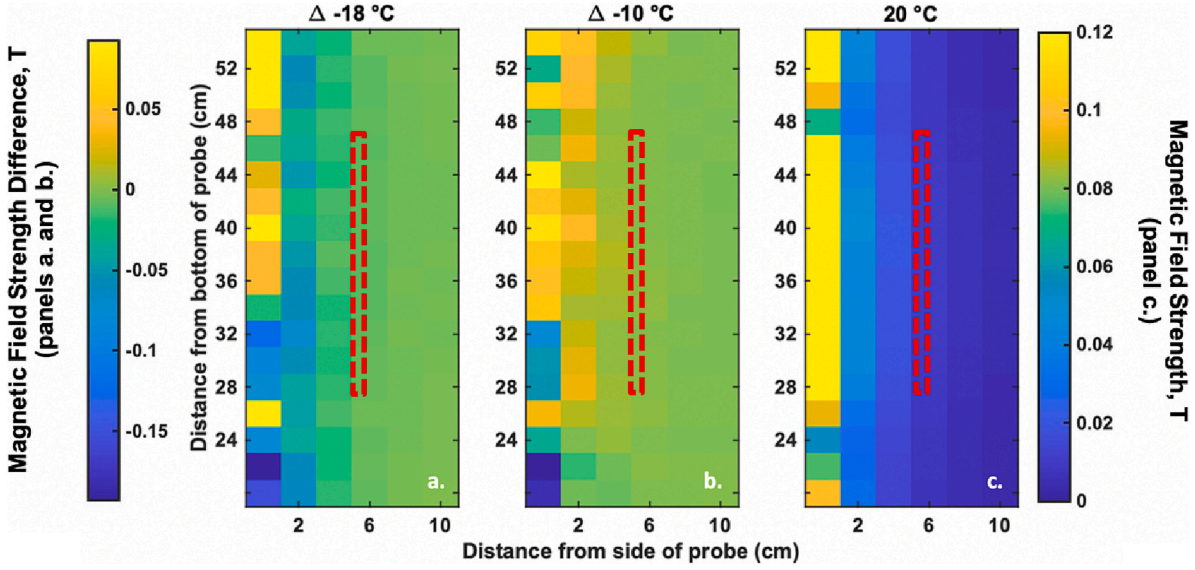

Fig. 4. Magnetic field strength differences (a. and b.) relative to room temperature borehole-NMR field strength (c.) shown for 10 °C and −8 °C. The radial cross-section of the zone of sensitivity is indicated by red dashed box. (For interpretation of the references to colour in this figure legend, the reader is referred to the web version of this article.)

content remained stable ($\theta_{\mathrm{NMR,\ mean}} = 109\%$; $\theta_{\mathrm{NMR,\ standard\_deviation}} = 1.4\%$).

5. Discussion

This investigation informs the effect of temperature on NMR measurements in freezing soils by assessing the question: How does temperature affect NMR measurements under the circa-cryotic conditions of permafrost active layer soils? In this research, we establish that borehole NMR water content calibrations change up to 18% with 20 °C temperature changes. The following sections place these observations in the context of the science questions of this study and relevant research.

5.1. NMR temperature dependence in bulk water

The NMR net magnetization of water depends on sample temperature, the number of water molecules within the sensitive zone, magnetic field strength, and temperature-independent physical constants. This study shows a temperature dependence of 0.9% $^{\circ}C^{-1}$ in borehole NMR measurements on bulk water. This temperature dependence is greater than that which is approximated by fundamental relationships, 0.4% $^{\circ}C^{-1}$.

5.2. The effects of a cold magnet

Exaggerated NMR water content at low temperature might be explained by magnetic field strength temperature dependence. As in H1

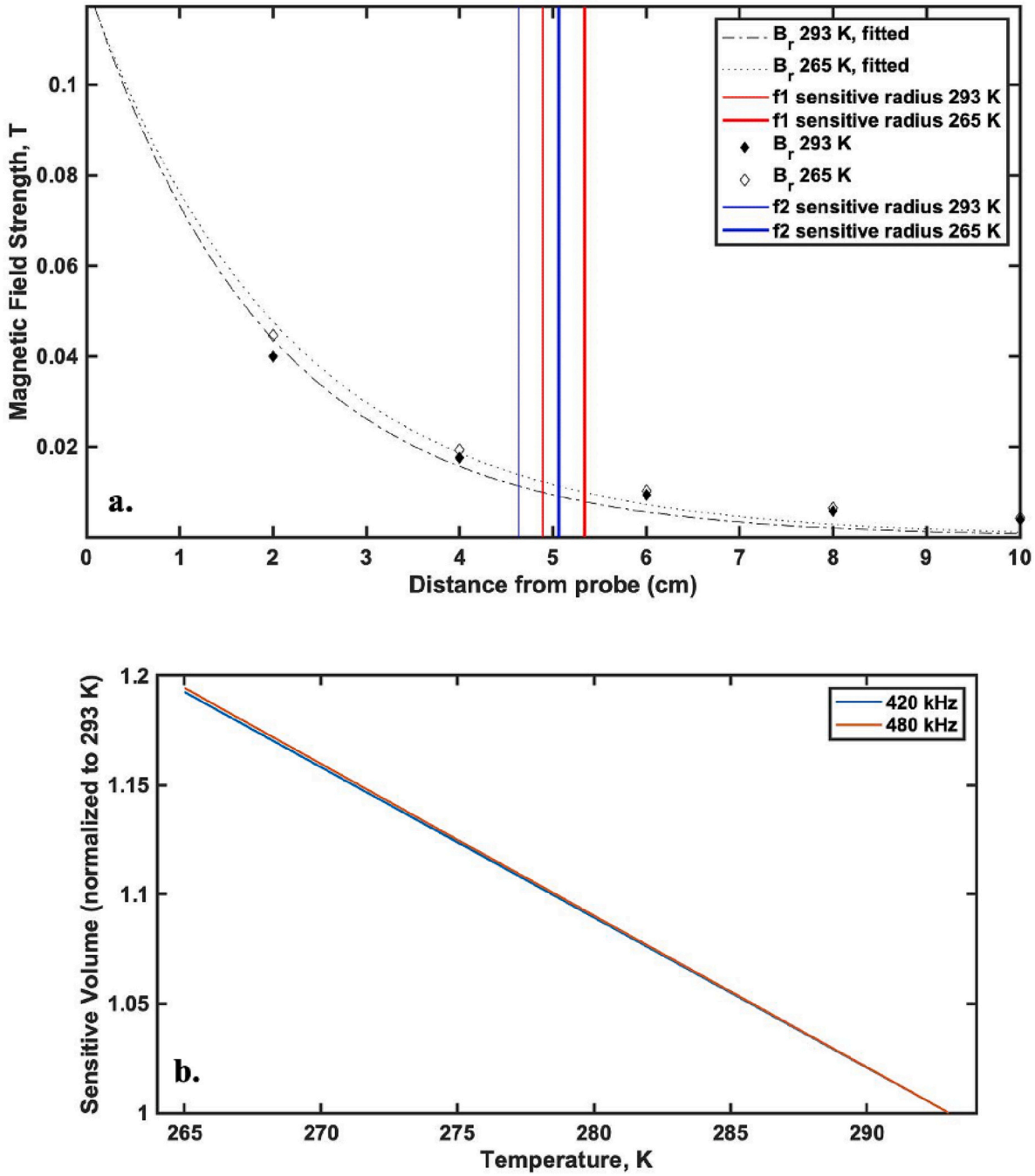

Fig. 5. Magnetic field strength as a function of distance from the NMR probe with marked sensitive distances at 20 °C and − 8 °C (a), and sensitive volume of borehole-NMR as a function of temperature (b).

and H2, cooling of the rare earth magnet within the probe is expected to increase magnetic field strength and result in a sensitive volume with a larger radius from the probe and therefore greater total sensitive volume relative to the calibration conditions (Fig. 2). We observe that the measured borehole NMR data (open circle markers in Fig. 2) acquired when both the probe and water were simultaneously cooled nearly align with the model displaying the predicted increase in sensitive volume due to reduced magnet temperature (Fig. 2 and Fig. 5a). However, further testing exploring the effect of separate cooling of the water and probe cast doubt on this explanation. When the magnet temperature alone was varied (i.e., probe cooled while insulated from water held at constant temperature), the observed NMR water content did not change (Fig. 6), casting doubt on H1 and H2. We note that the results of the magnet-cooling experiment encountered somewhat higher noise conditions (~6%, Fig. 6) compared to the experiment when the probe and water were cooled together (~3.5% Fig. 1), and we therefore recognize that it is possible that unexpected noise prevented us from observing the temperature effect on the magnetic field strength.

5.3. *Temperature dependent diffusion*

We attribute the temperature dependance of the NMR signal in part to the reduced self-diffusion of water at cooler temperatures (Nakashima, 2004) in support of H3. Nakashima (2004) observed pulsed NMR responses from bentonite clay at temperatures spanning 11 °C to 70 °C and water contents from 0 to 37.7% by weight—finding that T_1, T_2, and

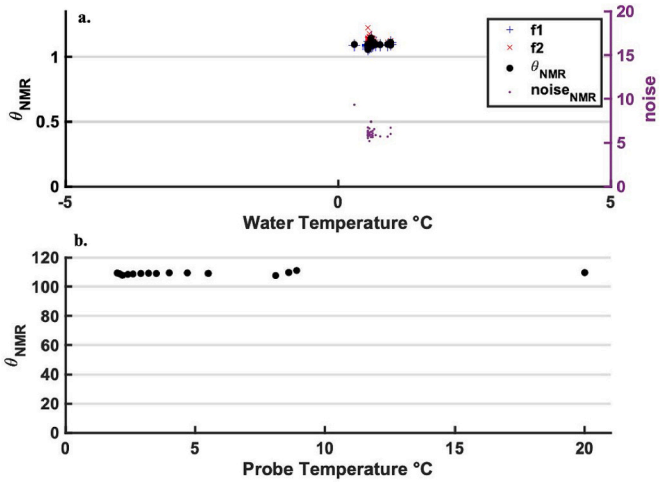

Fig. 6. NMR response with varying probe temperature. (a) shows (i) NMR-water contents derived from NMR frequencies f1 and f2–426,270 Hz and 478,271 Hz, respectively, (ii) the weighted average of the frequency-specific water contents, and (iii) the total noise in the NMR spin echo decay curve (reported as % on the right axis). Fig. 6b. shows the NMR-reported water contents as a function of probe temperature.

D (the diffusion coefficient of H_2O) increased with increasing temperature.

Due to molecular movement and magnetic field gradients within background magnetic fields, sample magnetization diminishes over time, and this effective decay is known as diffusion (Grebenkov, 2007; Kleinberg and Horsfield, 1990). The self-diffusion coefficient is influenced by water molecule surroundings as well as thermal characteristics (Grebenkov, 2007; Holz et al., 2000). If the magnetic field heterogeneities surrounding the borehole NMR probe (Fig. 4) are significant, the sensitive volume may not change with magnetic temperature as posed by H1 and H2—this would agree with the influence of magnetic field heterogeneities and Brownian motion of water (Kleinberg and Horsfield, 1990).

Modelling the impact of water density on NMR signal ($Model_{standard}$ vs. $Model_{density}$ in Fig. 4) suggests that the 1% increase in density with decreasing water from 20 °C to 0 °C has minimal impact on NMR measurements over these temperatures (Eq. (4)). Other possible explanations for exaggerated NMR water content include diffusive, i.e. Brownian, motion of water protons or non-linear magnetic field gradients as in H3 (Grebenkov, 2007). The temperature effects evident in NMR measurements in freezing soils emphasize the need for temperature-specific calibration values in field applications [Q1].

Measurements in this study agree with previous NMR experiments on temperature sensitivity and emphasize the instrument dependence of NMR temperature sensitivity (Akagawa et al., 2012; Kruse et al., 2018). The temperature dependence of the signal amplitude is instrument-specific according to both literature and the findings of this study. This NMR-instrument-specific calibration line resembles the calibration line introduced by Tice et al. (1981) advocating a similar temperature-specific NMR calibration relating FID intensity to sample temperature (A. Tice et al., 1982; A. R. Tice et al., 1981). The precise reason(s) for the instrument-specific signal amplitude to temperature relationships remains unknown. One possible reason for instrument-specificity may be differences in magnetic field sources and permanent magnet orientations; magnetic field gradients are sensitive to these variables and affect diffusion (Fig. 3, (Carr and Purcell, 1954; Kleinberg and Horsfield, 1990; Meiboom and Gill, 1958)).

5.4. Practical considerations for temperature accounting in borehole NMR

Because (1) fluctuations in surface temperature yield steep temperature gradients in active layer soil profiles and (2) the calibration of NMR measurements depends on temperature, NMR-assessment of active layer soils should employ a temperature-dependent calibration correction specific to each instrument. In NMR applications within the active layer, the temperature of the sample at the time of measurement should be recorded or modeled.

Findings from this study demonstrate that lower temperatures yield a bias of ~18% in NMR responses in liquid water for a sample at 0 °C using a calibration for 20 °C. This results in overestimated water contents in near-saturation soils if sample temperature is not considered. The overestimation is relative to measured water content and depends on the difference between the measurement temperature and calibration temperature. For example, if the true volumetric liquid water content in an unsaturated soil was 0.100 $m^3\ m^{-3}$ measured at 0 °C the calibration was conducted at 20 °C, the NMR observation would reflect the 18% overestimation report water content of 0.118 $m^3\ m^{-3}$, an error of 0.018 $m^3\ m^{-3}$. In contrast, consider a nearly saturated peat soil with true water content of 0.8 $m^3\ m^{-3}$ measured at 0 °C with the calibration conducted at 20 °C, the NMR observation would report water content of 0.944 $m^3\ m^{-3}$, an error of 0.144 $m^3\ m^{-3}$. In the former case, the error may be within the measurement noise (typically 2–3%) and be inconsequential; however, in the latter case it would be critical to account for the temperature effect to obtain reliable results.

5.5. Soil temperature compensation method

We advocate use of a temperature correction factor in each borehole NMR profile where the magnitude of the sample temperature difference in degrees exceeds the value of the NMR signal noise in %. In the case of many field applications with the Dart, 3% noise is frequently observed, and therefore a temperature-difference tolerance of 3 °C is suggested for this instrument. For such instances where the temperature difference is known or suspected to exceed this tolerance (as in most active layer applications), we recommend the following steps:

1. Measure the temperature of the soil profile

For one-time measurements without a nearby temperature profile readily available, we advise deploying a temporary thermistor string with thermistors at measurement depths of the NMR sensitive zone. This thermistor string should equilibrate to the ground temperatures for 12 to 24 h before recording the temperature profile. Attaching a thermistor to the side of the probe near the sensitive zone is ill advised due to: (i) the probe temperature is not as important as the ground temperature (Fig. 6), and (ii) the wait time for the probe temperature to equilibrate to the surrounding ground temperature would tremendously slow data collection efforts.

For time lapse measurements on established boreholes, we recommend deploying a logging thermistor string (with sensors at depths of NMR measurements) and using temperature profile data from the time of measurements for NMR signal corrections. Borehole NMR measurements may be conducted within fluid filled, established logging wells given that the sensitive zone of the instrument exists entirely outside of the disturbed zone of the boreholes. Turbulent borehole fluids displaced by the instrument probe will not affect NMR measurements given that the sensitive zone of the instrument exists outside of the borehole. A removable thermistor string may be deployed within fluid filled, established logging wells as fluid within these wells will adopt a similar temperature profile to the well surroundings. For continual, repeat measurements at a study site, we recommend deploying a logging thermistor string adjacent to- but outside of the sensitive zone of the measurement profile remains a best practice as it requires few

assumptions and extra steps during data acquisition.

2. Determine the temperature dependence

The temperature dependance on borehole NMR measurements should be treated as an instrument-specific correction factor, and therefore a calibration temperature model (e.g., Fig. 3) should be developed for each field instrument before or after a field experiment. To determine the temperature correction factor for a specific NMR instrument, one should conduct calibration measurements on a stagnant water sample at 0 °C and 20 °C. The equation of a line intersecting these points will equal the temperature correction function. For the Dart, the temperature correction function is the linear fit of normalized NMR water content in bulk water as in Fig. 3.

3. Scale NMR sensed water contents to temperature

After observing the subsurface temperature profile and establishing the instrument temperature dependence, one can determine the necessity of a temperature correction factor on NMR sensed water contents. Should such a correction be necessary, scale the reported NMR sensed water contents using the equation of the line, i.e. the temperature correction function, described in the previous paragraph.

6. Conclusion

We conclude that the temperature effect on NMR signals is not negligible, particularly in permafrost active layer investigations where steep temperature gradients as a function of depth may be encountered, and large seasonal soil temperature variations are expected. The instrument-specific temperature correction factor can be developed and applied based on field measured temperature data. This study is limited to the effect of temperature on NMR signal amplitudes and does not consider NMR relaxation time distributions in permafrost measurements. The effect of temperature on NMR relaxation times (observed previously in clays) likely manifests in active layer studies and remains an outstanding research question for future NMR investigations. Constraining the effects of temperature on NMR signatures will allow for more reliable NMR inspection of hydrogeochemical parameters in permafrost ecosystems such as ice content, geochemical observations such as iron speciation, evidence of biological activity like biofilms, and hydraulic parameters like conductivity and fluid flows, among others. Such hydrobiogeochemical observations are critical as researchers continue to observe and model multiple facets and feedbacks of warming permafrost ecosystems.

Funding

This work was supported by the National Science Foundation [grant number: 1829100], the University of Wyoming AAPG Weimer Family Grant, and the University of Wyoming Paul Crissman Arts and Sciences Scholarship.

CRediT authorship contribution statement

Taylor D. Sullivan: Conceptualization, Investigation, Formal analysis, Validation, Methodology, Writing – original draft, Resources. **Andrew D. Parsekian:** Conceptualization, Supervision, Formal analysis, Writing – review & editing, Visualization, Investigation, Resources, Funding acquisition.

Declaration of Competing Interest

The authors declare that they have no known competing financial interests or personal relationships that could have appeared to influence the work reported in this paper.

Data availability

Data used to support findings of this study are available from the corresponding author upon request.

Acknowledgements

We thank Mathew Elliot at University of Wyoming for assistance with data acquisition. Anna Wagner, Tom Douglas, Art Gelvin, and Jon Maakestad at the United States Army Corps of Engineers Cold Regions Research and Engineering Lab's Alaska Research Office provided critical logistical support for this study.

Appendix A. Supplementary data

Supplementary data to this article can be found online at https://doi.org/10.1016/j.coldregions.2023.103850.

References

Akagawa, S., Iwahana, G., Watanabe, K., Chuvilin, E., Istomin, V., 2012. Improvement of pulse-nmr technology for determining the unfrozen water content in frozen soils. In: Hinkel, K. (Ed.), Proceedings of the Tenth International Conference on Permafrost, vol. 1.

Anderson, D.M., Tice, A.R., 1973. The unfrozen interfacial phase in frozen soil water systems. In: Hadas, A., Swartzendruber, D., Rijtema, P.E., Fuchs, M., Yaron, B. (Eds.), Physical Aspects of Soil Water and Salts in Ecosystems, vol. 4. Springer, Berlin Heidelberg, pp. 107–124. https://doi.org/10.1007/978-3-642-65523-4_12.

Behroozmand, A.A., Keating, K., Auken, E., 2015. A Review of the Principles and applications of the NMR Technique for Near-Surface Characterization. Surv. Geophys. 36 (1), 27–85. https://doi.org/10.1007/s10712-014-9304-0.

Bloch, F., 1946. Nuclear induction. Phys. Rev. 70 (7–8), 460.

Brown, R., Gamson, B., 1960. Nuclear magnetism logging. Trans. AIME 219 (01), 201–209.

Carr, H.Y., Purcell, E.M., 1954. Effects of Diffusion on Free Precession in Nuclear magnetic Resonance experiments. Phys. Rev. 94 (3), 630–638. https://doi.org/10.1103/PhysRev.94.630.

Douglas, T.A., Turetsky, M.R., Koven, C.D., 2020. Increased rainfall stimulates permafrost thaw across a variety of Interior Alaskan boreal ecosystems. NPJ Clim. Atmosph. Sci. 3 (1), 28. https://doi.org/10.1038/s41612-020-0130-4.

Grebenkov, D.S., 2007. NMR survey of reflected Brownian motion. Rev. Mod. Phys. 79 (3), 1077–1137. https://doi.org/10.1103/RevModPhys.79.1077.

Ground Water Manual Hydrologic Data and Internet Resources, 1977. In: Fierro Jr., P., Nyler, E.K. (Eds.), The Water Encyclopedia, 3rd ed. U.S. Department of the Interior, Bureau of Reclaimation.

Holtzer, A.M., 1954. The collected papers of Peter. J. W. Debye. J. Polym. Sci. 13 (72), 700. https://doi.org/10.1002/pol.1954.120137203.

Holz, M., Heil, S.R., Sacco, A., 2000. Temperature-dependent self-diffusion coefficients of water and six selected molecular liquids for calibration in accurate 1H NMR PFG measurements. Phys. Chem. Chem. Phys. 2 (20), 4740–4742. https://doi.org/10.1039/b005319h.

James, S.R., Minsley, B.J., McFarland, J.W., Euskirchen, E.S., Edgar, C.W., Waldrop, M. P., 2021. The biophysical role of water and ice within permafrost nearing collapse: insights from novel geophysical observations. J. Geophys. Res. Earth Surf. 126 (6) https://doi.org/10.1029/2021JF006104.

Jorgenson, M.T., Osterkamp, T.E., 2005. Response of boreal ecosystems to varying modes of permafrost degradation. Can. J. For. Res. 35 (9), 2100–2111. https://doi.org/10.1139/x05-153.

Kass, M.A., Irons, T.P., Minsley, B.J., Pastick, N.J., Brown, D.R.N., Wylie, B.K., 2017. In situ nuclear magnetic resonance response of permafrost and active layer soil in boreal and tundra ecosystems. Cryosphere 11 (6), 2943–2955. https://doi.org/10.5194/tc-11-2943-2017.

Kleinberg, R.L., Griffin, D.D., 2005. NMR measurements of permafrost: Unfrozen water assay, pore-scale distribution of ice, and hydraulic permeability of sediments. Cold Reg. Sci. Technol. 42 (1), 63–77. https://doi.org/10.1016/j.coldregions.2004.12.002.

Kleinberg, R.L., Horsfield, M.A., 1990. Transverse relaxation processes in porous sedimentary rock. J. Magnet. Reson. (1969) 88 (1), 9–19. https://doi.org/10.1016/0022-2364(90)90104-H.

Kruse, A.M., Darrow, M.M., Akagawa, S., 2018. Improvements in measuring unfrozen water in frozen soils using the pulsed nuclear magnetic resonance method. J. Cold Reg. Eng. 32 (1), 04017016. https://doi.org/10.1061/(ASCE)CR.1943-5495.0000141.

Meiboom, S., Gill, D., 1958. Modified spin-echo method for measuring nuclear relaxation times. Rev. Sci. Instrum. 29 (8), 688–691. https://doi.org/10.1063/1.1716296.

Minsley, B.J., Pastick, N.J., Wylie, B.K., Brown, D.R.N., Andy Kass, M., 2016. Evidence for nonuniform permafrost degradation after fire in boreal landscapes: mapping postfire permafrost degradation. J. Geophys. Res. Earth Surf. 121 (2), 320–335. https://doi.org/10.1002/2015JF003781.

Müller-Petke, M., Yaramanci, U., 2015. Tools and techniques: Nuclear magnetic resonance. In: Treatise on Geophysics, 2nd ed., pp. 419–445.

Nakashima, Y., 2004. Nuclear magnetic resonance properties of Water-Rich Gels of Kunigel-V1 Bentonite. J. Nucl. Sci. Technol. 41 (10), 981–992. https://doi.org/10.1080/18811248.2004.9726321.

Rabi, I.I., 1937. Space quantization in a gyrating magnetic field. Phys. Rev. 51 (8), 652.

Romanovsky, V.E., Osterkamp, T.E., 2000. Effects of unfrozen water on heat and mass transport processes in the active layer and permafrost. Permafr. Periglac. Process. 11 (3), 219–239. https://doi.org/10.1002/1099-1530(200007/09)11:3<219::AID-PPP352>3.0.CO;2-7.

Smith, M.W., Tice, A.R., 1988. Measurement of the Unfrozen Water Content of Soils: Comparison of NMR and TDR Methods.

Tian, H., Wei, C., Lai, Y., Chen, P., 2018. Quantification of water content during freeze-thaw cycles: a nuclear magnetic resonance based method. Vadose Zone J. 17 (1), 160124 https://doi.org/10.2136/vzj2016.12.0124.

Tice, A.R., Burrous, C.M., Anderson, D.M., 1978. Determination of unfrozen water in frozen soil by pulsed nuclear magnetic resonance, pp. 149–155. https://go.exlibris.link/6hlgYvkL.

Tice, A.R., Anderson, D.M., Sterrett, K.F., 1981. Unfrozen water contents of submarine permafrost determined by nuclear magnetic resonance. Eng. Geol. 18 (1–4), 135–146. https://doi.org/10.1016/0013-7952(81)90053-3.

Tice, A., Oliphant, J., Nakano, Y., Jenkins, T., 1982. Relationship between the Ice and Unfrozen Water Phases in Frozen Soil as Determined by Pulsed Nuclear Magnetic Resonance and Physical Desorption Data, 82–15. U.S. Army Cold Regions Research and Engineering Lab, p. 15.

Tice, A., Black, P., Berg, R., 1988. Unfrozen Water Contents of Undisturbed and Remolded Alaskan Silt as Determined by Nuclear Magnetic Resonance (CRREL Report No. 88–19; p. 23). US Army Corps of Engineers.

Van Everdingen, R.O., 1998. Multi-Language Glossary of Permafrost and Related Ground-Ice Terms in Chinese, English, French, German, Icelandic, Italian, Norwegian, Polish, Romanian, Russian, Spanish, and Swedish. International Permafrost Association, Terminology Working Group.

Waller, I., 1932. Über die Magnetisierung von paramagnetischen Kristallen in Wechselfeldern. Z. Phys. 79 (5), 370–388.

Walsh, D., Turner, P., Grunewald, E., Zhang, H., Butler, J.J., Reboulet, E., Knobbe, S., Christy, T., Lane, J.W., Johnson, C.D., Munday, T., Fitzpatrick, A., 2013. A small-diameter NMR logging tool for groundwater investigations: D. Walsh ground water xx, no. xx: xx-xx. Groundwater 51 (6), 914–926. https://doi.org/10.1111/gwat.12024.

Watanabe, K., Wake, T., 2009. Measurement of unfrozen water content and relative permittivity of frozen unsaturated soil using NMR and TDR. Cold Reg. Sci. Technol. 59 (1), 34–41. https://doi.org/10.1016/j.coldregions.2009.05.011.

Wlostowski, A.N., Gooseff, M.N., Adams, B.J., 2018. Soil moisture controls the thermal habitat of active layer soils in the McMurdo dry valleys, Antarctica. J. Geophys. Res. Biogeosci. 123 (1), 46–59. https://doi.org/10.1002/2017JG004018.